Modeling and validation of high-performance and athermal AWGs for the silicon photonics platform

Stefano Tondini[a,b], Claudio Castellan[a], Mattia Mancinelli[a], and Lorenzo Pavesi[a]

[a]Nanoscience Laboratory, Department of Physics, University of Trento, Via Sommarive 14, 38123, Trento, Italy
[b]Dipartimento di Fisica, Informatica e Matematica Universita' di Modena e Reggio Emilia,, Via Campi 213/a, 41125, Modena, Italy

ABSTRACT

Array waveguide gratings (AWGs) are a key component in WDM systems, allowing for de-multiplexing and routing of wavelength channels. A high-resolution AWG able to satisfy challenging requirements in terms of insertion loss and X-talk is what is needed to contribute to the paradigm change in the deployment of optical communication that is nowadays occurring within the ROADM architectures. In order to improve the performances and keep down the footprint, we modified the design at the star coupler (SC) and at the bending stages. We evaluated how the background noise is modified within a whiskered-shaped SC optimized to reduce the reflectivity of the SOI slab and keep down back-scattered optical signal. A dedicated heating circuit has also been designed, in order to allow for an overall tuning of the channel-output. A high-performance AWG has also to cope with possible thermal-induced environmental changes, especially in the case of integration within a Photonic Integrated Circuit (PIC). Therefore, we suggested a way to reduce the thermal-sensitivity.

Keywords: Star coupler, Fabry-Perot interference, Heating circuit, A-thermal design, Array Waveguide Grating, Wavelength Division Multiplexing, Silicon on Insulator.

1. INTRODUCTION

Optical filtering devices can be realized by means of integrated Photonics, benefiting of its low footprint and low cost. Several configurations have been demonstrated as the AWGs or the micro-resonator based de/multiplexer matrix.[1,2,3] Today, after more than 20 years of continued research, AWGs are one of the most important filter type applied in WDM networks, and the advance of PIC technology is going to boost them even more.[4] In the WDM scheme, multiple sources are modulated and encoded to carry optical signals. The data rate for each channel is limited by the modulation speed. Anyway, the total bandwidth can be scaled by the number of wavelengths (channels) used in the optical communication system via a high-resolution AWG able to get over the performances achieved so far.[5,6,7] In order to improve the design, we developed a novel SC, a dedicated heating circuit and a compensation strategy to face with temperature variations.

2. EXPERIMENTAL

In this section we are going to explain in detail the different apporaches followed to improve the AWG design.

2.1 Star Coupler Reflectance Reduction

In order to reduce the interface reflectivity within the SC stage, we realized a modified SC by placing, perpendicularly to the focal lines, a series of inverse tapered waveguides, which end in a particular geometry, acting as "reflection killers". The Finite Element Method (FEM) simulation of the electric field profile propagating through the "reflection killer" geometry is shown in (Fig.1 (c)). Estimated back reflection are about $-18\ dB$. We evaluate the background noise within a standard SC (Fig.1 (a)) and within a whiskered-shaped one (Fig.1 (b)). The study has been carried out by analysing the Fabry-Perot (FP) interference that arises between the

Further author information: (Send correspondence to Stefano Tondini)
Stefano Tondini: E-mail: stefano.tondini@unitn.it, Telephone: +39 0461 282906

Silicon Photonics and Photonic Integrated Circuits V, edited by Laurent Vivien, Lorenzo Pavesi, Stefano Pelli,
Proc. of SPIE Vol. 9891, 98910C · © 2016 SPIE · CCC code: 0277-786X/16/$18 · doi: 10.1117/12.2227511

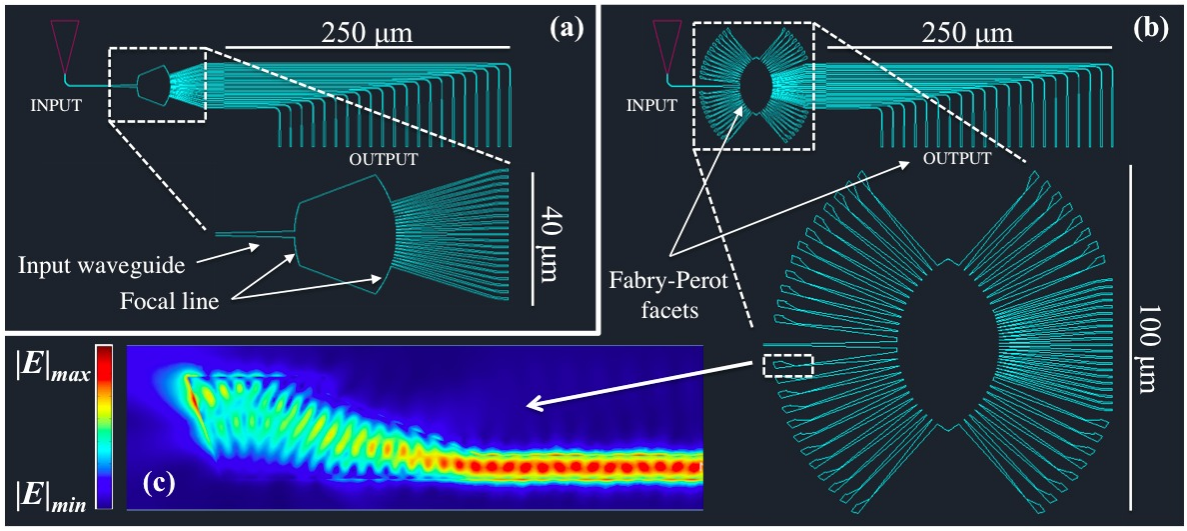

Figure 1. (a) Standard SC with 1 input waveguide and 21 output waveguides. (b) Whiskered SC with 1 input waveguide and 21 output waveguides. (c) FEM simulation of the electric field profile propagating through the "reflection killer" geometry.

input focal line of the SC and the output facet of a waveguide (indicated in Fig.1).[8] We compared the performances of the whiskered SC with respect to the standard one, taking into account the spectra collected from the same output waveguide of the two analyzed devices.

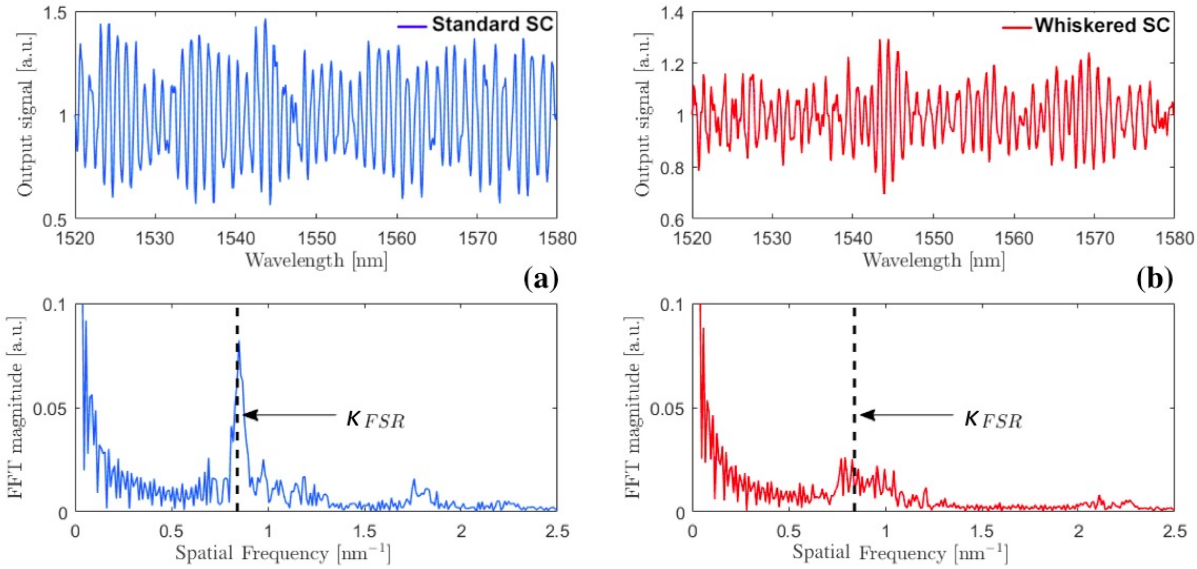

Figure 2. (top - a and b) Fabry-Perot (FP) interference evaluated by injecting a tunable IR laser within both the structures showed in Fig.1(a) and (b). We identified as the FP facets the input focal line of the SCs and the ending facets of the waveguide of the array. (bottom - a and b) FFT performed on the experimental spectra. The dashed line represents the spatial frequency predicted by FP theory.

FP oscillations have larger amplitude for the standard design, as can be seen in the top plots of Fig.2. This is pointed out also by the FFT of the spectra, which peaks at about the same frequency but differs in magnitude.

From the FP theory, we expect the free spectral range $\Delta\lambda_{FSR}$ to be described by:

$$\Delta\lambda_{FSR} = \frac{1}{\kappa_{FSR}} = \frac{\lambda_0^2}{2Ln_g}, \tag{1}$$

where λ_0 is the wavelength at which constructive interference occurs, L is the distance between the reflective facets and n_g is the group index of the mode within the cavity. n_g is the weighted average calculated on both the SC and the output waveguide group indices, obtained by mode analysis simulations. The dashed line in figure Fig.2 (bottom plots) represents the spatial frequency predicted by inverse of the relation 1, computed for a wavelength of 1550 nm.

By evaluating the peak amplitude of FFT performed on the optical spectra, we have been able to compare the performances of the whiskered SC with respect to the standard one. In particular, we related the reflectivity of the standard SC, found by simulation of a SOI slab ending in silica, with the reduced reflectivity of wishkered SC, due to the presence of the "reflection killers". We evaluate the reflectance of the two SC designs, by averaging on the values obtained for the FP spectra from the different output waveguides. We find a reflectance value for the whiskered SC of $(9 \pm 1) \times 10^{-3}$, which is more than one order of magnitude lower than the reflectance value of the standard SC, about 0.18.

2.2 Bezier Bends

Usally the bends in the SOI devices are realized in a width that avoids exciting high order modes. For this reason, the waveguides are inverse tapered before the bending and tapered after. This is detrimental for the footprint, since an adiabatic tapering could take several tens of microns.

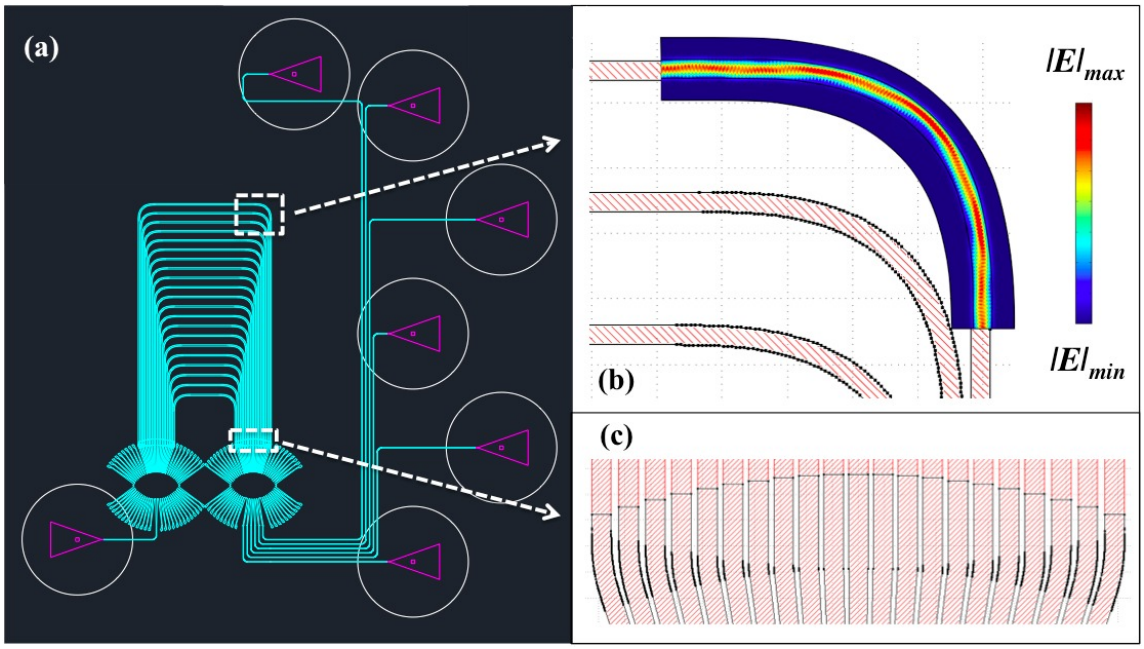

Figure 3. (a) AWG layout: in cyan the silicon waveguides, in magenta the grating couples. (b) FEM simulation of the electric field profile propagating through the Bezier bending geometry realized for minimizing the footprint. (c) Bezier bendings adopted instead of circular arcs at the SC/array junction.

To fix this problem, i.e. to reduce the footprint, we decided to attempt an AWG design (Fig.reffig:fig3 (a)) where the circular arc bends have been replaced with Euler's curves (3 (b) and (c)). This geometry has a curvature that changes linearly with the curve length, making the bending the less abrupt as possible.[9] Calculations show that, for a 1.5 μm width waveguide, the bending losses in a 90 ° Euler's curve with a radius of 15 μm are below 0.05 dB, and that high order modes are not significantly excited. With this geometry, there is no need

of a tapering stage before and after the bending of the AWG, and this reduces dramatically the footprint. The parametric equation of the Euler's bend implemented within the design routine are:

$$\begin{cases} x = \int_0^\tau \frac{A\sqrt{2}}{2}\tau^{-\frac{1}{2}}\cos(\tau)d\tau \\ y = \int_0^\tau \frac{A\sqrt{2}}{2}\tau^{-\frac{1}{2}}\sin(\tau)d\tau \end{cases} \tag{2}$$

where A accounts for the scaling factor and τ is the deviation angle. Such a parameterization leads to a clothoid curve. Therefore we designed the first half of the curve, for example up to a τ value of 45 °, and we obtained the second half by reverse mirroring the previous one.

2.3 Heating circuit

Several configuration of AWG heating systems have been already demonstrated, but due to the robustness of AWG to the fabrication errors, especially in the array waveguides, a huge amount of power is needed for the tuning.[10] In addition to the other improving strategies describer so far, we realized a fine-tuning heating circuit by covering a section of the AWG waveguides with a series of Ti/TiN strips (Fig.4 (a)). The result is shown in Fig.4 (b) and in Fig.4 (c) is reported the equivalent circuit, consisting in a set of resistances of the same value, connected in parallel. This geometry guaranties a uniform current density in each vertical strip of the heater. Since these vertical strips have been chosen in such a way that the length difference between two adjacent strips remains constant, when the heater is biased each waveguide of the array undergoes an optical path enlargement proportional of its own length. This, in turn, makes the difference between two adjacent waveguides remaining the same, also during the heating. The shifting efficiency has been estimated being around 3 nm/W for a Ti/TiN heating layer of $5.5 \div 6\ \Omega/sq$ placed $600nm$ above the SOI waveguides. What has to be noticed is that the horizontal connection rectangles (in the middle of the heating circuit) become more and more wide with increasing the number of waveguides to be heated. Therefore, this design is suitable for low-footprint and low-waveguides number AWGs.

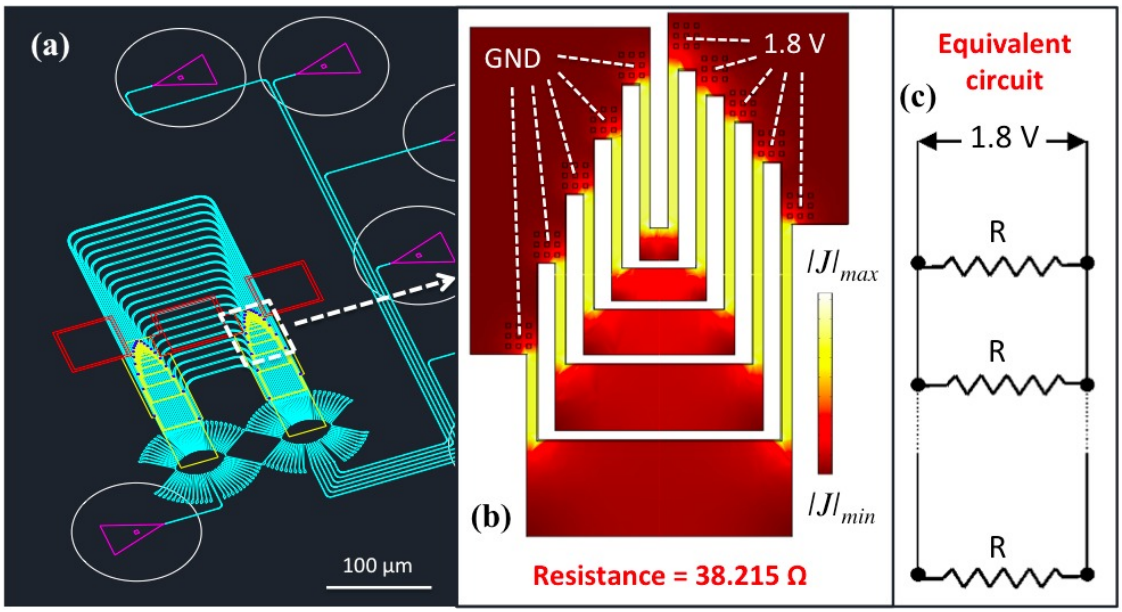

Figure 4. (a) AWG layout with heating elements: in cyan the silicon waveguides, in magenta the grating couples, in yellow the Ti/TiN heaters, in blue the copper vias, in red the electric pads (b) FEM simulation of current density through the heater when the bias is switched on. (c) Equivalent circuit where it can be seen that the strips have been dimensioned to obtain the same resistance value for each arm.

2.4 A-thermal design

An important requirement for an AWG is its stability with respect to temperature changes. For reducing thermal dependence of the AWG output, it is possible to replace the silica cladding, that has a small thermo-optic coefficient (TOC), with a different material sharing negative TOC.[11] The temperature variations affect the refractive index, which, as a function of temperature T can be written as:

$$n(\lambda, T) = n_0(\lambda) + \kappa(T - T_0)\,, \tag{3}$$

where $n_0(\lambda)$ is the usual refractive index dispersion relation at the reference temperature T_0 and κ is the TOC. The simulated spectrum of the first output channel of an AWG at different temperature is shown in Fig.5 (a). As can be seen, the spectrum is red-shifted as a consequence of the temperature increase. In Fig.5 (b) is reported the experimental output channel peak shift as a function of the temperature (blue scattered data). The shift appears to be linear, with a shift per unit of temperature $\frac{\Delta\lambda}{\Delta T}$ of about 80 pm/K (the simulation, blue solid line, is in a good agreement with the experimental data).

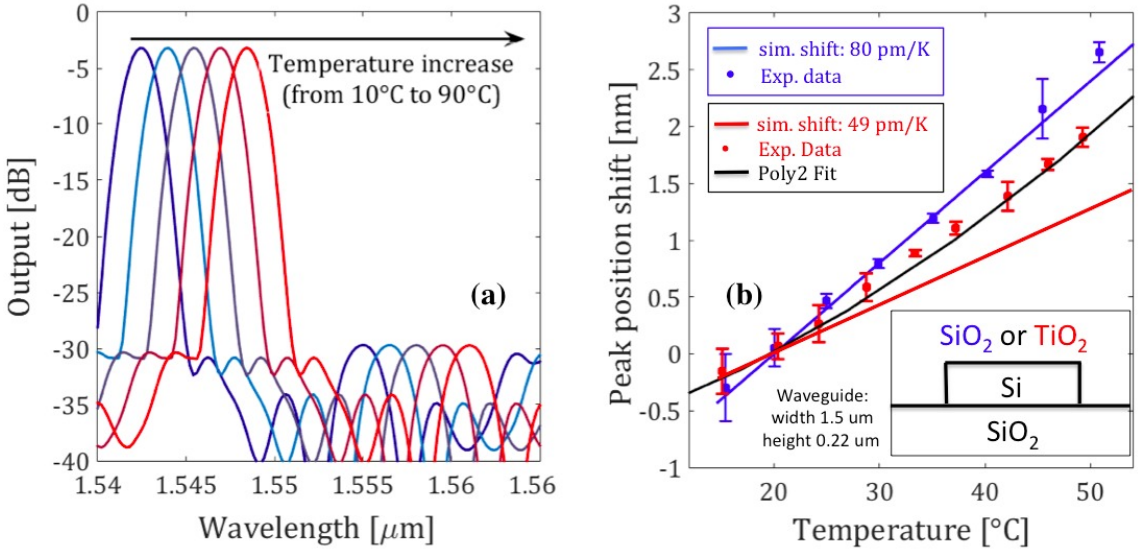

Figure 5. (a) Simulated output spectrum of the outer channel of the AWG design when the temperature undergoes a temperature variation from 280 K to 360 K. (b) Comparison between the peak position shift due to temperature variation in the case of array waveguides with silica cladding (blue solid line), and titania cladding (red solid line). Experimental measurements are also reported. In the case of the experimental data from the tiania covered AWG the quadratic fit is also represented. In the inset is sketched the waveguide cross section (not to scale) with the fabrication paramenters.

The maximum temperature variation that the device can undergo is therefore related to the largest spectrum shift allowed (it depends on how much stringent are the requirements with respect to the transmission grid). A possible choice for reducing the thermal effects is substituting SiO_2 cladding with TiO_2, a CMOS-compatible material whose TOC value depends on deposition technique. For example, using evaporation techniques, titania TOC varies from $-5 \times 10^{-4} K^{-1}$ to $-7 \times 10^{-4} K^{-1}$ with hysteresis.[12] Simulations of an AWG sharing the same design parameters as the previous one, but with a TiO_2 cladding (TOC of $-5 \times 10^{-4} K^{-1}$) are reported with a solid red line in Fig.5 (b). In this case, the experimental results, the red scattered data, are not compatible with the theoretical prediction. Also the trend seems to be quadratic instead of linear, as can be seen by the second order polynomial fit performed on the experimental data. A possible explanation of this particular behaviour could be found, in our opinion, by analysing the fabrication process of the TiO_2 cladding. Despite this fact, the substitution of silica with titania allows for a reduction of temperature shift, at least in the case of small temperature variations.

3. ACHIEVEMENTS

In this work, we address an improved suppression of the edge-reflected light in the whiskered SC. We developed a model, which, on the basis of the scattering matrix theory, well fits the experimental results. This approach can be a useful tool to be exploited also for other photonic devices where special attention has to be paid to the interferential noise that affect the free propagation of beams. By means of Bezier bends in the place of circular arc bends we suggest a way to reduce the footprint of the AWG design. Moreover we dimensioned a heating circuit that allows the fine-tuning of the AWG channel-output. By applying specific phase-shifts on each single waveguide of the array we have been able to move the FSR without affecting the channels spacing. The suggested geometry minimizes the power consumption needed to obtain an appreciable wavelength-shift in the AWG output spectrum. We committed also in adjusting the temperature-dependent wavelength shift that the waveguides undergo when a temperature variation is experienced by the AWG. We simulated and realized a design using a cladding material with a negative thermo-optic coefficient. By means of a TiO_2 covering, we reduced the thermal sensitivity of the whole device.

ACKNOWLEDGMENTS

The research leading to these results has received funding from the European Union's Seventh Framework Programme (FP7/2007-2013) under grant agreement n 619194.

REFERENCES

[1] Venghaus, H., [*Wavelength filters in fibre optics*], vol. 123, springer (2006).

[2] Bogaerts, W., Dumon, P., Van Thourhout, D., Taillaert, D., Jaenen, P., Wouters, J., Beckx, S., Wiaux, V., and Baets, R. G., "Compact wavelength-selective functions in silicon-on-insulator photonic wires," *Selected Topics in Quantum Electronics, IEEE Journal of* **12**(6), 1394–1401 (2006).

[3] Xu, Q. and Soref, R., "Reconfigurable optical directed-logic circuits using microresonator-based optical switches," *Opt. Express* **19**, 5244–5259 (Mar 2011).

[4] F. Testa, e. a., "Design and implementation of an integrated reconfigurable silicon photonics switch matrix in iris project," *Selected Topics in Quantum Electronics, IEEE Journal of* (2016).

[5] Pathak, S., Vanslembrouck, M., Dumon, P., Van Thourhout, D., and Bogaerts, W., "Optimized silicon awg with flattened spectral response using an mmi aperture," *Lightwave Technology, Journal of* **31**(1), 87–93 (2013).

[6] Cheung, S., Su, T., Okamoto, K., and Yoo, S., "Ultra-compact silicon photonic 512× 512 25 ghz arrayed waveguide grating router," *Selected Topics in Quantum Electronics, IEEE Journal of* **20**(4), 310–316 (2014).

[7] Pathak, S., Van Thourhout, D., and Bogaerts, W., "Design trade-offs for silicon-on-insulator-based awgs for (de) multiplexer applications," *Optics letters* **38**(16), 2961–2964 (2013).

[8] Chen, C.-L., [*Foundations for guided-wave optics*], John Wiley & Sons (2006).

[9] Cherchi, M., Ylinen, S., Harjanne, M., Kapulainen, M., and Aalto, T., "Dramatic size reduction of waveguide bends on a micron-scale silicon photonic platform," *Optics express* **21**(15), 17814–17823 (2013).

[10] Yang, Y., Hu, X., Song, J., Fang, Q., Yu, M., Tu, X., Lo, G.-Q., et al., "Thermo-optically tunable silicon awg with above 600 ghz channel tunability," *Photonics Technology Letters, IEEE* **27**(22), 2351–2354 (2015).

[11] Padmaraju, K. and Bergman, K., "Resolving the thermal challenges for silicon microring resonator devices," *Nanophotonics* **3**(4-5), 269–281 (2014).

[12] Lee, J.-M., "Influence of titania cladding on soi grating coupler and 5μm-radius ring resonator," *Optics Communications* **338**, 101–105 (2015).